Magnetically Tunable Fiber Bragg Grating Supported by Guiding Mechanism System

Heba A. Fayed (hebam@aast.edu), **Mohamed Mahmoud** (m.mahmoud@aast.edu),
A.K. AboulSeoud[1] (Aboul_Seoud_35@yahoo.com) and **Moustafa H. Aly**[2] (drmosaly@gmail.com)

Arab Academy for Science, Technology and Maritime Transport, Alexandria, Egypt.
[1] Faculty of Engineering, University of Alexandria, Egypt.
[2] OSA Member.

ABATRACT

A Bragg grating fast tunable filter prototype working over a tuning range of 62 nm has been realized. The tunable fiber Bragg grating TFBG system is achieved by varying an input current to a solenoid, resulting in an electromagnetic force, used as a strain (tension and compression) on the FBG. However, during compression, the FBG may be subject to buckling especially when the amount of compression is large. The challenge for the FBG device is therefore to design guiding system for the FBG in order to prevent the buckling. This paper presents the design of such a guiding system. These novel TFBG devices with a guiding system can have a variety of applications in optical fiber communication systems; such as programmable optical add/drop multiplexers (OADMs), dispersion compensators and tunable lasers.

Keywords: Tunable fiber Bragg grating, guiding system, buckling, electromagnetic force, strain.

1. INTRODUCTION

A fiber Bragg grating (FBG) is a periodic perturbation of the refractive index along the fiber length which is formed by exposure of its core to an intense interference light pattern. Hill et al. [1] in 1978 first noticed permanent changes in the refraction index of germanium-doped optical fibers due to an intense argon-ion laser irradiation launched into the fiber. Various methods [2] are today in use to fabricate Bragg gratings by exposure of the fiber to ultraviolet (UV) laser light as the interferometric [3] and the phase mask techniques [4]. Photo-induced FBGs are currently in use for example as mirrors for fiber lasers [5], as temperature, stress or pressure fiber sensors in engineering [6], as filters, mode converters [7] or wavelength multiplexers in telecommunications [3].

To shift the grating central wavelength peak, there are two main methods: by modifying the fiber refractive index or by changing the grating period. These variations can be induced thermally [8, 9] or by mechanical stresses [9–12]. Due to the excellent silica behavior under stress and its low thermal expansion coefficient, 10–11 pm/^{o}C at 1.5 μm, mechanical stresses have been preferentially applied to obtain wide tuning ranges. Compression is more preferable since silica fiber can withstand much larger compressive stress than tensile stress [11]. To achieve a long wavelength tuning range as possible, compression of the FBG is an effective method. However, during compression, the FBG may be subject to buckling especially when the amount of compression is large. The challenge for the FBG device is therefore to design a guiding system which is shown in this paper. This paper sets up the following specific objectives. First, to design a device to tuning the Bragg wavelength shift up to 62 nm with a guiding system to avoid buckling which is proposed and described in Sec. 2. The second objective is to develop some analytical equations analyzing the guiding system design given in Sec. 3. A parallel wide band TFBG design using our tunable device is presented in Sec. 4, followed by the conclusion in Sec. 5.

Photonics North 2010, edited by Henry P. Schriemer, Rafael N. Kleiman, Proc. of SPIE Vol. 7750,
77501Z · © 2010 SPIE · CCC code: 0277-786X/10/$18 · doi: 10.1117/12.871525

2. DEVICE DESCRIPTION

A schematic diagram of the magnetically TFBG device is shown in Fig. 1. The device consists of two steel closely spaced programmable magnets (solenoids), with dimensions of L = 10 cm long and 2 cm in diameter. The solenoids have 5000 turns and could produce a magnetic flux density of B = 0.754 T with a current of 120 mA at the initial separation between the two magnets x = 1.85 cm. One of the programmable magnets is fixed and the other is movable. The movable programmable magnet is attached to the fiber which includes 10 mm of FBG and its other end is attached to a lockable system.

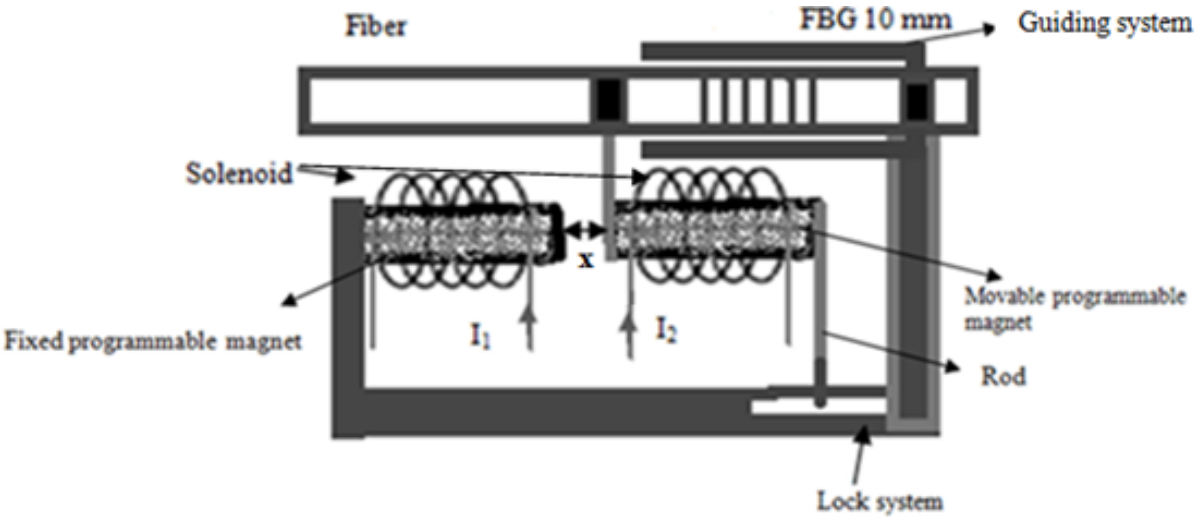

Fig. 1 Schematic of magnetically-tunable fiber Bragg grating.

The fiber containing the Bragg grating is epoxy bonded on one side of the grating to the movable magnet and is fixed on the other side. It is inserted in a guiding system to avoid buckling. The programmable magnets are then magnetized in a controllable manner using input currents I_1, I_2 such that the two magnets are magnetically attractive or repulsive and move closer or away from each other. This in turn strains the FBG by a tension or a compression, respectively, and shifts the Bragg grating wavelength.

A key advantage of this approach is that once the programmable magnets are magnetized, no continuous supply of power is needed to achieve the set shift. This is due to the lock system, as the movable magnet is bounded by a rod; this rod moves freely when current is applied (tuning the wavelength shift) and stuck (hold its place) when there is no current. This reserve the shift gained in the TFBG system when no current is applied.

3. DESIGN THEORY FOR GUIDING SYSTEM

The fiber grating wavelength shift is given by [11]

$$\Delta\lambda_B = \lambda_B.(1-P_e).\ \varepsilon \qquad (1)$$

where λ_B is the Bragg wavelength and P_e is the effective strain-optic constant defined as [11]

$$P_e = \frac{n_{eff}^2}{2}.\{P_{12} - \nu(P_{11} + P_{12})) \quad (2)$$

where P_{11} and P_{12} are components of the strain-optic tensor, and ν is the Poisson's ratio. For a typical silica optical fiber $P_{11} = 0.153$, $P_{12} = 0.273$, $\nu = 0.17$, and $n_{eff} = 1.5$. Using these parameters, $P_e = 0.22$ [13, 14]. $\varepsilon = \Delta L / L$ is the axial strain (tensile or compressive) imposed on the FBG. For a wavelength shift of -49.608 nm, the required axial compression strain change ε will be around 4 %.

3.1 FBG Strain Ranges

Typical mechanical properties of FBG are indicated in Fig. 2. Although a tensile breaking strength of an optical fiber without writing the grating is up to 6000 MPa, it drops to about 700 MPa during the grating process [11]. The tensile strength is reduced by the fiber exposure to high intensity UV radiations during manufacturing using phase mask technique, which is being widely used to manufacture FBGs due to its simplicity. The 700 MPa tensile strength gives a tension strain of only around 1%, which can theoretically give a wavelength shift of about 12 nm according to Eq. (1).

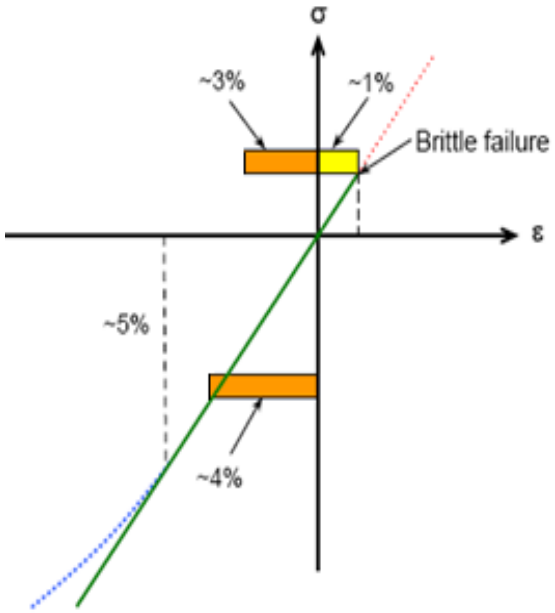

Fig. 2 Stress-strain relationship for an optical fiber [12].

Typically, an optical fiber is up to 20 times stronger in compression than that in tension. Also, a compression strain up to 5% is linear as shown in Fig. 2. In this system, to achieve the 5% needed strain that gives an overall shift in Bragg wavelength of 62 nm, only 1 % of tension can be applied as shown in Fig. 3. Therefore, the reaming 4% is achieved from the compression strain. The only technical problem is that it is very difficult to compress a thin optical fiber because of buckling so that we add a guiding system to avoid buckling.

3.2 Design Theory

From the buckling theory, a fiber of an unguided length L_b (also referred to as the buckling length) and a geometrical moment of inertia (I), will buckle if the critical value compressive force (F_{cr}) is [13]

$$F_{cr} = \frac{\pi^2 \, EI}{L_b^2} \tag{3}$$

where E is the modulus of elasticity of fiber material (= 72.5 GPa for silica).

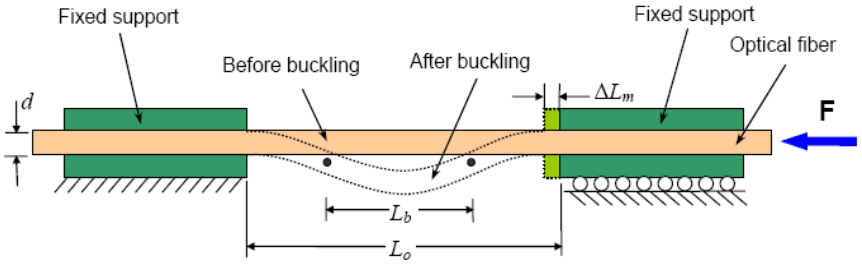

Fig. 3 Buckling of FBG under compression.

The critical stresses σ_{cr} can be calculated as

$$\sigma_{cr} = \frac{F_{cr}}{A} = \frac{\pi^2 \, E \, i^2}{L_b^2} = \frac{\pi^2 \, E}{S^2} \tag{4}$$

where A is the cross-sectional area of fiber core ($=\pi d^2/4$), i is the radius of gyration of fiber ($i^2 = I/A = d^2/16$), S is the slenderness ($= L_b / i = L_b / (I/A)^{1/2} = 4\, l_b / d$).

The critical strain ε_{cr} will be

$$\varepsilon_{cr} = \frac{\sigma_{cr}}{E} = \frac{\pi^2}{S^2} = \frac{\pi^2 d^2}{16 L_b^2} \tag{5}$$

Rearranging Eq. (5), the maximum unsupported buckling length for a given axial strain can be written as:

$$L_b = \frac{\pi d}{4\sqrt{\varepsilon_{cr}}} \tag{6}$$

If both ends of the FBG are fixed as shown in Fig. 4, then $L_b = 0.5\, L_o$, where L_o is the length of FBG, typically about 10 mm. For L_o = 10 mm, the amount of compressive strain that can be carried without buckling of an optical fiber of 125 μm diameter is only about 0.038%, which is much less than the required strain (4%) as shown in the previous section. On the other hand, to carry an axial compressive strain of 4% without buckling, the unguided length should not be greater

than 0.49 mm. Therefore, it is clear that a fiber guiding system is needed in order to achieve the required strain without buckling of the fiber.

3.3 FBG Supported by Cylindrical Guiding

A simple way of guiding the unsupported FBG is with the help of a cylindrical guiding. The ends of the FBG will be glued to the cylindrical guiding as shown in Fig. 4-a. Inside the cylindrical guiding, the fiber will buckle but its lateral deflection will be limited by the gap (D – d), where D is the inside diameter of the cylindrical guiding and d, as before, is the diameter of the fiber. Some clearance (ΔL) will be required between the cylindrical guiding and the moving fixed bound for the required compression.

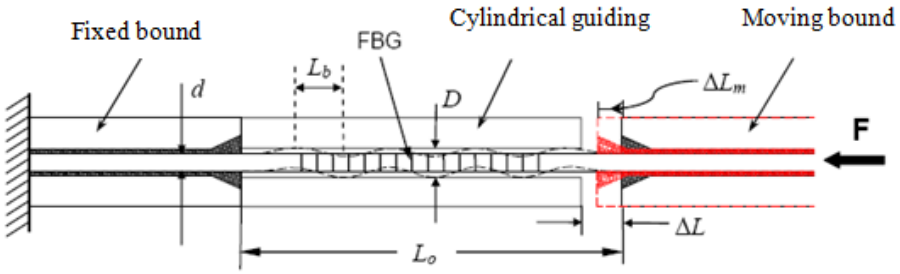

Fig.4-a. Support for unguided region under compression.

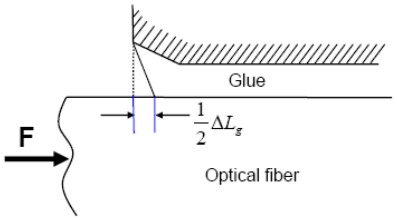

Fig.4-b. Deformation of glue.

The axial strain in the fiber, ε_{ax}, will be monitored by measuring the displacement, ΔL_m, of the moving bound on the right hand side. The measured displacement results from the combination of the axial compression of the FBG, ΔL_{ax}, the shortening due to waving of the optical fiber, ΔL_w, and the deformation of the epoxy, ΔL_g, as shown in Fig.4-b. So

$$\Delta L_m = \Delta L_{ax} + \Delta L_w + \Delta L_g \tag{7}$$

The measured axial strain, ε_m, is defined as

$$\varepsilon_m = \frac{\Delta L_m}{L_0} = \varepsilon_{ax} + \varepsilon_w + \varepsilon_g \tag{8}$$

Theoretically, the clearance between the internal diameter, D, of cylindrical guide and the fiber diameter, d, should be as small as possible to minimize buckling to achieve a minimum optical power loss from the optical fiber. But, this is practically impossible due to Poisson's effect. In particular, the tolerance of both d and D below ±1 μm is expensive to achieve. A large clearance may result in significant optical power loss. Therefore, some compromise is required in which

acceptable results can be achieved with a reasonable manufacturing cost. As will be discussed, the range of D from 126 to 128 μm seems acceptable to guide a 125 μm fiber.

The relationship of the cost of manufacturing versus the tolerance is shown in Fig. 5.

3.4 Stresses in Fiber

The optical fiber inside the cylindrical guide will buckle under a compressive force causing axial and lateral deformations. For a strain ε_{ax}, the average axial compressive stress, σ_c, is given by

$$\sigma_c = - \varepsilon_{ax} E \tag{9}$$

According to structural stability theory [13], the axial strain in the fiber (of length L_b) at the moment of buckling remains almost unchanged, i.e. $\varepsilon_{ax} \approx \varepsilon_{cr}$, as long as the deflections are moderate.

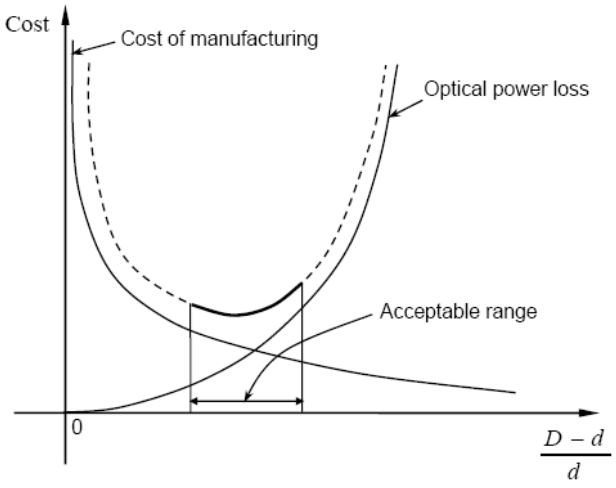

Fig. 5 Factors affecting the cylindrical guide design.

The bending stresses can be estimated by assuming that the buckling takes place in one plane as shown in Fig. 6.

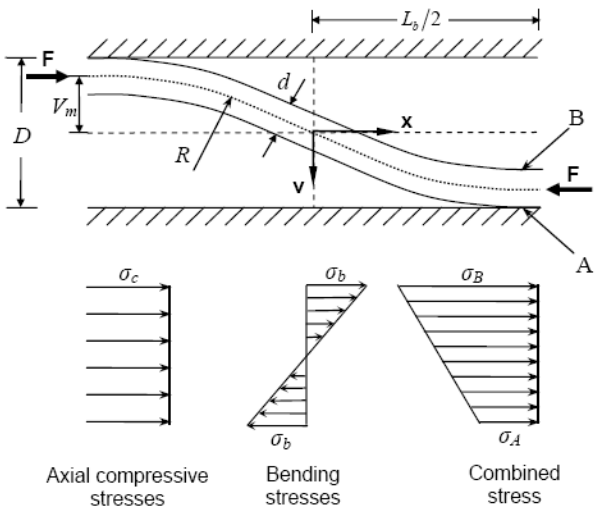

Fig. 6 Stress distribution in fiber under compression.

From bending theory, the buckling radius, R, is related to the bending moment, M, by [13]

$$\frac{1}{R} = \frac{d^2v}{dx^2} = \frac{M}{EI} \tag{10}$$

The buckled shape can be assumed to be

$$v = V_m \sin\left[\frac{\pi x_b}{L_b}\right] \tag{11}$$

where V_m= (D - d)/2 is the wave's amplitude and L_b is its length that depends on the axial strain. Substituting Eq.(11) into Eq.(10), the maximum bending moment at $x_b = L_b/2$ is

$$\frac{M_{max}}{EI} = V_m \frac{\pi^2}{L_b^2} \tag{12}$$

and the corresponding maximum bending stress is

$$\sigma_b = \pm\frac{M_{max}d}{2I} = \pm E\frac{V_m d\pi^2}{2L_b^2} = \pm 4E\left[\frac{D}{d} - 1\right]\varepsilon_{ax} \tag{13}$$

Point B of the fiber will be under compressive bending stresses and point A will be under tensile bending stresses. From Eq. (9) and Eq. (13), the combined stress at point A is:

$$\sigma_A = \sigma_c + \sigma_b = -E\varepsilon_{ax} + 4E\left[\frac{D}{d} - 1\right]\varepsilon_{ax} = \varepsilon_{ax}E\left[\frac{4D}{d} - 5\right] \tag{14}$$

and the combined stress at point B is:

$$\sigma_B = \sigma_c - \sigma_b = -E\varepsilon_{ax} - 4E\left[\frac{D}{d} - 1\right]\varepsilon_{ax} = -\varepsilon_{ax}E\left[\frac{4D}{d} - 3\right] \tag{15}$$

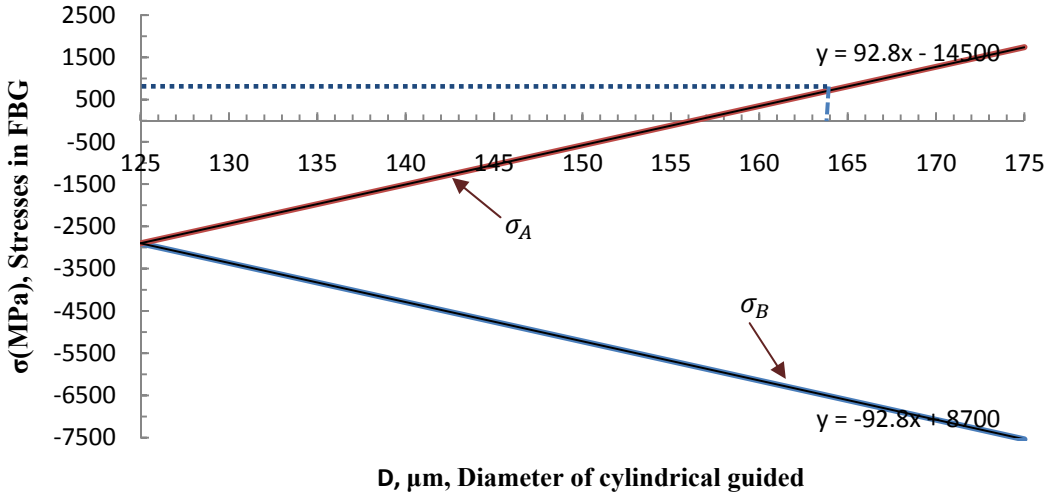

Fig. 7 Stresses of FBG with the internal diameter of the cylindrical guide.

For an optical fiber diameter of 125 µm, a modulus of elasticity of 72.5 GPa and an axial strain of 4%, Eqs. (14) and (15) are plotted in Fig.7 in terms of the internal diameter, D, of the cylindrical guiding. It can be seen that for an internal diameter of 164 µm, the tensile stresses at point A will reach 700 MPa, which may cause the FBG to break. Theoretically, the stress at points A and B will be identical for D = d. Note that when D = 127 µm, the stresses at both point A and B are compressive.

3.5 Effect of Curvature on FBG Performance

Light waves transmit through an optical fiber due to total internal reflection as shown in Fig. 8. Bending of the optical fiber causes them to escape from the core of the optical fiber because of change in the reflection and refraction angels of the light waves. The escape of light waves from the core results in optical power loss. The larger the curvature of the fiber the more will be the optical power loss.

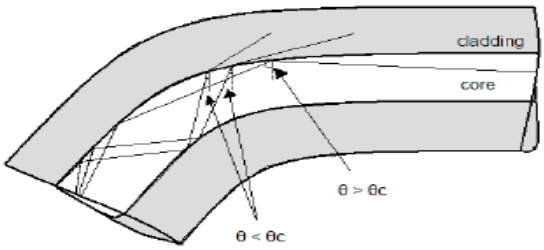

Fig. 8. Optical power loss due to bending.

The minimum radius of curvature of the fiber inside the cylindrical guide can be obtained by letting M in Eq.(10) as M_{max} and substituting Eq.(12) into Eq.(10), yielding

$$R_{min} = \frac{L_b^2}{V_m \pi^2} = \frac{1}{8\varepsilon_{ax}} \frac{d^2}{D-d} \tag{16}$$

Equation (16) is plotted in Fig. 9 for d = 125 μm and ε_{ax} = 4%. The figure shows how the radius of curvature of the fiber, R, is related to the internal diameter, D, of the guiding cylinder. The radius of curvature at which the stresses reach a breaking tensile stress value of 700 MPa is 1250 μm (1.25 mm), which makes the internal diameter of the cylindrical guide to be less than about 164 μm as illustrate in Fig. 7. Due to decrease in bending radius, the power loss will increase. This appears to be the upper limit of D that can be used in the guiding system design and must be less than 164 μm and lower limit of D must be greater than 125 μm. For example, if D = 127 μm, the minimum radius of curvature of the optical fiber inside the cylindrical guiding, calculated from Eq. (16), is 24.4 mm.

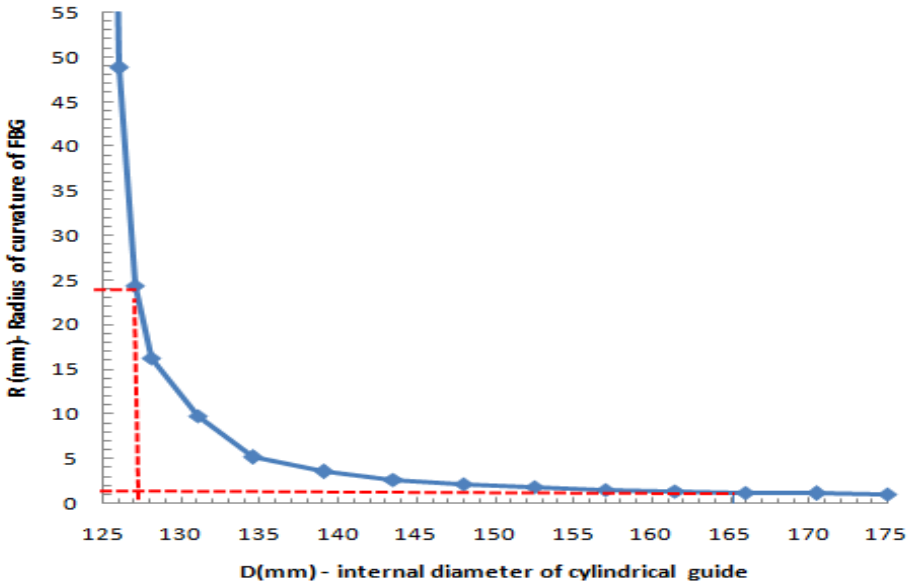

Fig. 9 Effects of internal diameter of the cylindrical guide on the bending radius.

Based on the theoretical analysis described above, the guiding system is designed for both axial stretch and compression of FBG. The TFBG design is basically divided into two systems: (1) A guiding system design which has been designed to minimize the bending of FBG under compression, and (2) A magnetically tunable design which achieves any required wavelength.

4. Parallel Wide Band TFBG Design

Figure 10 shows the proposed scheme of a wide band TFBG. The circuit includes two TFBGs (TFBG1, TFBG2) with a guiding system as discussed before, and the 3-port optical circulator (OC) integrates with the FBGs, which act as reflective mirrors to form a looped-back circuit. On the right hand side, there is one 1×2 optical switch (OSW) and two TFBGs connected to either output port of the OSW.

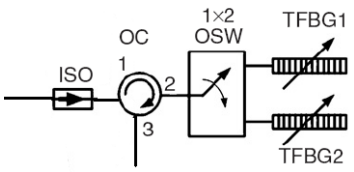

Fig.10. Parallel wide band TFBG design; OSW: optical switch, OC: optical circulator, TFBG: tunable fiber Bragg grating, ISO: optical isolator.

The TFBGs wavelengths were shifted to cover almost all of DWDM range. The first, TFBG1, begins from 1540 nm and has tunable ranges (from 1540 to 1490 nm in compression) and (from 1540 nm to 1552 nm in tension). The second, TFBG2, begins from 1602 nm and has tunable ranges (from 1602 nm to 1552 nm in compression) and (from 1602 nm to 1614 nm in tension). Using this configuration, one can get a wide tunable range (1490 to 1614 nm).

5. CONCLUSION

A developed design of a guiding system for axial compression of FBGs has been achieved including a TFBG system using an electromagnetic force controlled by applied current. The upper limit of D that can be used in the guiding system design must be less than 164 μm in order to avoid cutting the fiber and lower limit of D must be greater than 125 μm to avoid buckling. A wide wavelength tuning range of 62 nm is obtained. Also, an extension in the tuning range is achieved using a parallel wide band TFBG design to reach a tuning range of 124 nm. This tuning device is simple in configuration, low cost and easy to operate.

REFERENCES

[1] K. O. Hill, Y. Fujii, D. C. Johnson and B. S. Kawasaki, "Photosensitivity in optical fiber waveguides: application to reflection filter fabrication," Appl. Phys. Lett., vol. 32, pp. 647–649, 1978.

[2] G. Meltz, W. W. Morey and W. H. Glen, "Formation of Bragg grating in optical fibers by a transverse holographic method," Opt. Lett., vol. 14, pp. 823–825, 1989.

[3] I. Bennion, J. A. R. Williams, L. Zhang, K. Sugden and N. J. Doran, "UV-written in-fiber Bragg gratings," Optic. Quantum Electron., vol. 28, pp. 93–135, 1996.

[4] K. O. Hill, B. Malo, F. Bilodeau, D. C. Johnson and J. Albert, "Bragg gratings fabricated in monomode photosensitive optical fiber by UV exposure through a phase mask," Appl. Phys. Lett., vol. 62, pp. 1035–1037, 1993.

[5] H. G. Limberger, N. Hong Ky, D. M. Costantini, R. P. Salath´e, C. A. P. Muller and C. R. Fox, "Efficient active Bragg grating tunable filters," Proc. OFS '97, OSA Tech. Dig. Series, OSA Topical Meeting, Williamsburg, USA, 1997.

[6] G. A. Ball and W. W. Morey, "Tunable Bragg grating fiber filters and their applications," Proc. CLEO'97, Baltimore, MD, pp. 108–109, 1997.

[7] G. A. Ball and W. W. Morey, "Compression-tuned single-frequency Bragg grating fiber laser," Opt. Lett., vol. 19, pp. 1979–1981, 1994.

[8] M. M. Ohn, A. T. Alavie, R. Maaskant, M. G. Xu, F. Bilodeau and K. O. Hill, "Dispersion variable fiber Bragg grating using a piezoelectric stack," Electron. Lett., vol. 32, pp. 2000–2001, 1996.

[9] A. Iocco, H. G. Limberger and R. P. Salath´e, "Bragg grating fast tunable filter," Electron. Lett., vol. 33, pp. 2147–2148, 1997.

[10] P. Lambelet, P. Y. Fonjallaz, H. G. Limberger, R. P. Salath´e, Ch. Zimmer and H. H. Gilgen, "Tension and compression tuned Bragg grating filter," Proc. ECOC '98, Madrid, Spain, vol. 1, pp. 229–230, 1998.

[11] Monica L. Rocha, Flavio Borin, Hoan C.L. Monteiro, Mariza R. Horiuchi, Miriam R. X. de Barros, Maria Aparecida D. Santos, Flavia L. Oliveira and Fabio D. Simoes "Mechanical tuning of a fiber Bragg grating for optical network application," Journal of Microwaves and Optoelectronics, Brazilian Microwaves and Optoelectronics Society-SBMO, vol. 4, no. 1, pp. 1516-1527, June 2005.

[12] Jaroslav Mencik, “Strength and fracture of glass and ceramics,” Elsevier, New York, pp.1041-1048, 1992.
[13] N. Mohammad and W. Szyszkowski, “Analysis and development of a tunable fiber Bragg grating filter based on axial tension/compression", Journal of Lightwave Technol., vol. 22, no. 8, pp. 2001-2013, 2004.